A Model Predictive Control Strategy for the Cascaded H-Bridge Multilevel Rectifier Based on Enumeration

Petros Karamanakos, Konstantinos Pavlou, and Stefanos Manias
Electrical Machines and Power Electronics Laboratory
National Technical University of Athens (NTUA)
Iroon Polytechniou 9, 15780 Zografou, Athens, Greece
petkar@central.ntua.gr, kpavlou@central.ntua.gr, manias@central.ntua.gr

***Abstract*—In this paper model predictive control (MPC) is adapted for the cascaded H-bridge (CHB) multilevel rectifier. By directly manipulating the switches, the proposed control scheme aims to keep the input current in phase with the supply voltage, and to achieve independent regulation of the H-bridge cells. Furthermore, since all the possible switching combinations are taken into account, the controller exhibits favorable performance not only under nominal conditions, but also under asymmetrical voltage potentials and unbalanced loads. Finally, and in order to ensure robustness, a short horizon is employed; in that way the required computing remains reasonable, making it possible to implement the algorithm in a real-time system. Experimental results are presented in order to demonstrate the performance of the proposed approach.**

I. Introduction

Among the multilevel converters, the cascaded H-bridge (CHB) embodies the qualities of the most attractive topology in comparison with the neutral point clamp (NPC) and the flying capacitor (FC). The reasons for this are the minimum number of the switching devices, and the modularity which results to the ability of further expansion to higher levels. However, several issues are still open, specifically, when the topology is operated as a multilevel rectifier. In this mode of operation, the CHB rectifier aims to achieve n isolated dc buses, each of which may perform independently from the others, resulting in the need for more complex control strategies. In addition, the converter has to operate always under unity power factor with minimum power losses, while at the same time respecting the operational limits imposed by the topology [1]. Thus, numerous research works have been reported in literature.

Particularly, several control algorithms have been developed to maintain at most the requested demands. A high percentage of them rely on the multicarrier approach [2]–[5] which gives the benefit of constant switching frequency. Others use conventional [6] or generalized [7] modulation methods with low computation complexity exhibiting noteworthy performance. Furthermore, advanced control techniques employed in order to achieve various performance objectives, such as robustness and model parameter estimation. Specifically, for purposes of robustness, the sliding mode control [8], and the hysteresis current control [9], [10] are more suitable, while for the estimation of the model parameters the adaptive-passivity control [11] is ideal. For reasons of switching frequency reduction and power losses minimization, selective harmonic elimination pulse width modulation (SHE-PWM) control [12] is very promising.

Despite the effectiveness of the existing control approaches, there are still open tasks such as ease of controller design and elimination of tuning. Furthermore, the rapid development of fast microprocessors enabled the application of computationally demanding algorithms, such as model predictive control (MPC) [13], [14], to the field of power electronics. During the last decade this novel control strategy has been applied to several power electronics topologies [15]–[19], including the CHB converter operated as either an inverter [20], [21], or as a rectifier [22], with significant success.

MPC thanks to its straightforward implementation has achieved a lot of popularity. An objective function that incorporates the control objectives is formulated based on the mathematical model of the converter and it is minimized over the finite prediction horizon. The underlying optimization problem is solved in real-time; the optimal solution at each sampling instant is the sequence of control inputs that results in the best predicted behavior of the system. Only the first element of the optimal sequence is implemented. At the next step all the variables are shifted by one sampling interval and the complete procedure is repeated. This strategy, known as *receding horizon policy*, is employed in order to provide feedback.

In this work an MPC scheme for the CHB multilevel rectifier is proposed. In the inner loop, posed in the MPC framework, the input current is regulated to its sinusoidal reference, by directly manipulating the switches of the converter. An exhaustive search of all the possible switching combinations takes place resulting in a controller which is suitable to predict the behavior of the plant for a wide operation range. Furthermore, and in order to maintain the effectiveness of the controller under unbalanced output cell voltages, the deviation of the respective voltages from their references is taken into account. In that way the controller

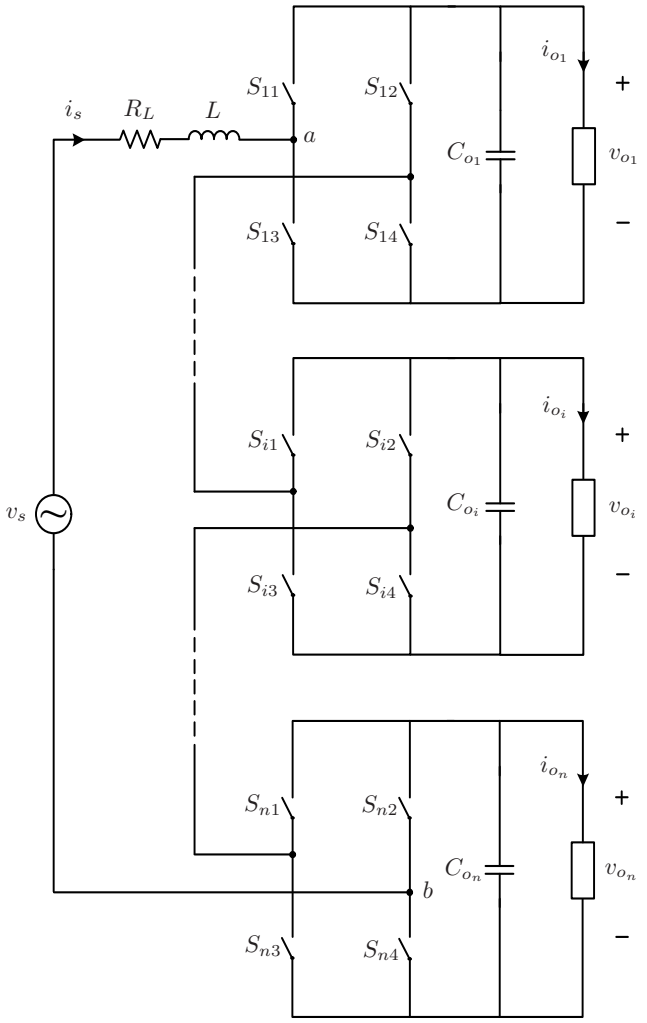

Fig. 1: Topology of the single-phase CHB multilevel rectifier consisting of n cells connected in series.

aims to reject all kind of disturbances, including load and output voltage variations.

A key benefit of the proposed algorithm is that despite its design simplicity it is capable of stabilizing the system for the entire operating regime. Furthermore, the control objectives are expressed in the objective function in a straightforward manner; in that way excessive tuning is avoided. Other advantages include the fast dynamics achieved by MPC. On the other hand the dominant drawback is that the computational power needed increases exponentially as the prediction horizon is extended. Moreover, the absence of a modulator and the direct manipulation of the converter switches imply a variable switching frequency.

This paper is organized as follows. In Section II the discrete-time model suitable for the controller is derived. The control objectives, the formulation of the optimization problem, and the proposed approach are presented in Section III. Section IV evaluates the performance of the proposed control approach by means of experimental results. Finally, the paper is summarized in Section V, where conclusions are drawn.

II. Model of the Cascaded H-Bridge Multilevel Rectifier

The topology of the CHB rectifier with n cells connected in series is illustrated in Fig. 1. The AC side consists of a boost inductance L, with internal resistor R_L. At the DC side each cell consists of a filter capacitor C_{o_i}, where $i \in \{1, 2, \ldots, n\}$ denotes the number of the cell, connected in parallel with the load.

Each H-bridge cell is composed of four switches S_{ij}[1], where $j \in \{1, \ldots, 4\}$ refers to the respective switch of the cell. The switches of each cell operate dually and in pairs denoted by T_{ip}, with $p \in \{1, 2\}$; the odd indexed switches (S_{i1} & S_{i3}) form one pair ($p = 1$) and the even indexed (S_{i2} & S_{i4}) the other ($p = 2$). The possible switching combinations of the ith cell of the converter are: $T_{i1}T_{i2} = 10$, $T_{i1}T_{i2} = 00$, $T_{i1}T_{i2} = 01$ and $T_{i1}T_{i2} = 11$, where "0" denotes the *off* state of the upper switch of the pair and "1" the *on* state.

The MPC controller is built around the discrete-time state-space model of the converter, which is derived by discretizing the continuous-time model using the forward Euler approximation approach. This yields:

$$x(k+1) = A_d(u)x(k) + B_d w(k) \tag{1a}$$
$$y(k) = C_d x(k)\,, \tag{1b}$$

where

$$x(k) = [i_s(k)\ v_{o_1}(k)\ \ldots\ v_{o_n}(k)]^T\,, \tag{2}$$

is the state vector, encompassing the inductor current and the output voltages of the individual cells. The input matrix $u(k) \in \mathbb{R}^{m\times m}$, with $m = n + 1$, is given by

$$u(k) = \begin{bmatrix} d_{i1} & 0 & \cdots & 0 & 0 \\ d_{i1} & 0 & \cdots & 0 & 0 \\ \vdots & \vdots & \ddots & \vdots & \vdots \\ d_{i1} & 0 & \cdots & 0 & 0 \\ 0 & d_{mi+1} & \cdots & d_{mi+1} & d_{mi+1} \end{bmatrix}, \tag{3}$$

where the entries of the matrix are

$$d_{i1} = d_{mi+1} = u_{i1} - u_{i2}\,. \tag{4}$$

The binary variable $u_{ip} \in \{0, 1\}$ is introduced in order to model the switching state of each dually operated pair of switches T_{ip}; $u_{ip} = 1$ refers to the case where $T_{ip} = 1$, and $u_{ip} = 0$ to the case being $T_{ip} = 0$. The input voltage $v_s(k)$ and the load current $i_{o_i}(k)$ of each cell form the vector of the disturbances $w(k) = [v_s(k)\ i_{o_1}(k)\ \ldots\ i_{o_n}(k)]^T$, while the respective output voltages are considered as the output, i.e.

$$y(k) = [v_{o_1}(k)\ \ldots\ v_{o_n}(k)]^T\,. \tag{5}$$

Finally the matrices are $A_d = (\mathbb{I} + A_1T_s + A_2T_s u(k))$, $B_d = T_s B$, and $C_d = C$, where $\mathbb{I}$ is the identity matrix, and T_s is the sampling interval, and the matrices A_1, A_2, $B \in \mathbb{R}^{m\times m}$ and $C \in \mathbb{R}^{n\times m}$ are given by

[1]Usually each switch is composed of an IGBT and an anti-parallel freewheeling diode.

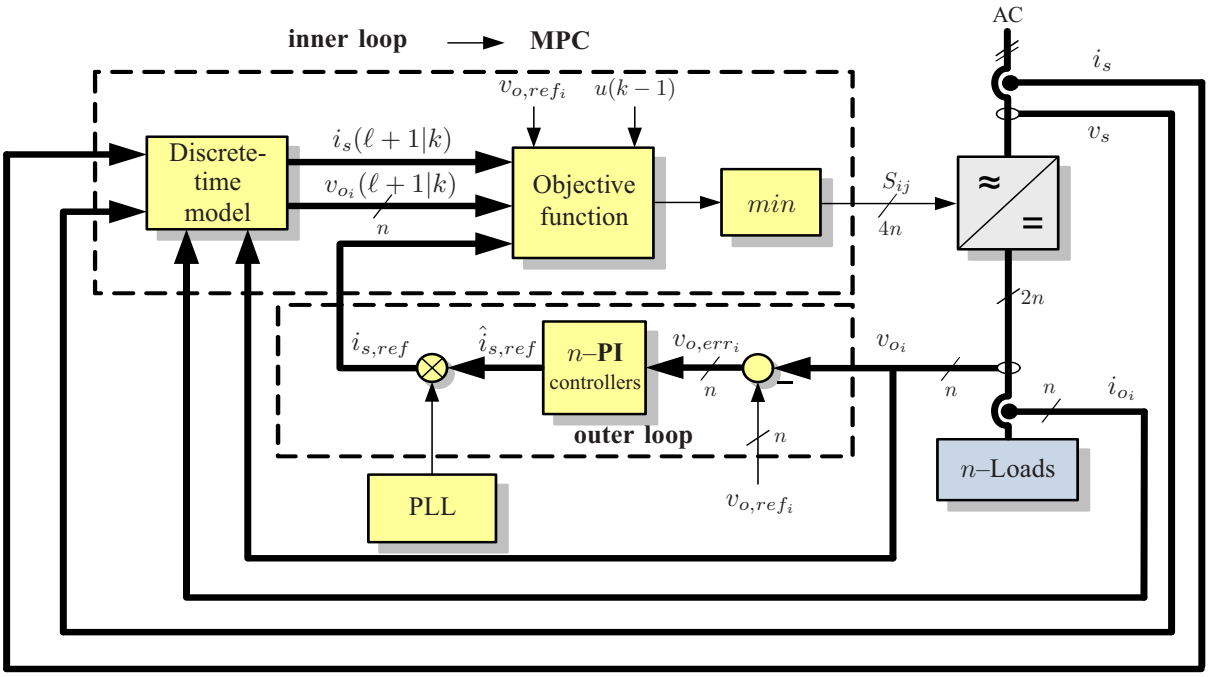

Fig. 2: Block diagram of the proposed model predictive control (MPC) scheme.

$$A_1 = \begin{bmatrix} -\frac{R_L}{L} & 0 & \cdots & 0 \\ 0 & 0 & \cdots & 0 \\ \vdots & \vdots & \ddots & \vdots \\ 0 & 0 & \cdots & 0 \end{bmatrix}, \tag{6}$$

$$A_2 = \begin{bmatrix} 0 & 0 & \cdots & 0 & -\frac{1}{L} \\ \frac{1}{C_{o_1}} & 0 & \cdots & 0 & 0 \\ 0 & \frac{1}{C_{o_2}} & \ddots & \vdots & \vdots \\ \vdots & & \ddots & 0 & 0 \\ 0 & \cdots & 0 & \frac{1}{C_{o_n}} & 0 \end{bmatrix}, \tag{7}$$

$$B = \text{diag}\Big(\frac{1}{L}, -\frac{1}{C_{o_1}}, \ldots, -\frac{1}{C_{o_{(n-1)}}}, -\frac{1}{C_{o_n}}\Big), \tag{8}$$

$$C = \begin{bmatrix} 0 & 1 & 0 & \cdots & 0 \\ 0 & 0 & 1 & 0 & \cdots \\ \vdots & \vdots & \ddots & \ddots & \vdots \\ 0 & 0 & \cdots & 0 & 1 \end{bmatrix}. \tag{9}$$

III. Control Problem and Approach

In this section an MPC scheme for the CHB multilevel rectifier is introduced. The input current is controlled by directly manipulating the switches of each cell; the respective output voltages are indirectly controlled. The proposed control algorithm is shown in the block diagram in Fig. 2.

A. Control Objectives

For the CHB multilevel rectifier the control objectives are multiple and of equivalent importance. Firstly the input current i_s of the topology should be sinusoidal and in phase with the supply voltage v_s, resulting in a unity power factor. Furthermore, the harmonic content of the current should be kept as low as possible with resulting in a low total harmonic distortion (THD), while simultaneously the switching frequency should remain low in order to reduce the switching losses. Finally, the output voltage of each cell v_{o_i} should accurately track its reference, and remain unaffected by changes in the load.

B. Optimal Control Problem

In the control method introduced here, the control problem is formulated as a current regulation problem, with the deviation of the inductor current from its reference defined as

$$i_{s,err}(k) = i_{s,ref} - i_s(k)\,. \tag{10}$$

Furthermore, in order to ensure that the output voltages of the rectifier cells will regulate to their references even when they are of different levels, the mean value of the respective error is calculated

$$v_{o,err}(k) = \frac{1}{n}\sum_{i=1}^{n} v_{o,ref_i} - v_{o_i}(k)\,. \tag{11}$$

Finally the difference between two consecutive switching states is penalized so as to decrease the switching frequency and avoid excessive switching according to

$$\Delta u(k) = u(k) - u(k-1)\,. \tag{12}$$

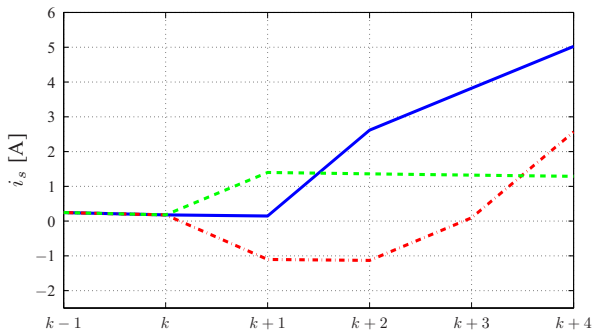

(a) Predicted current trajectories

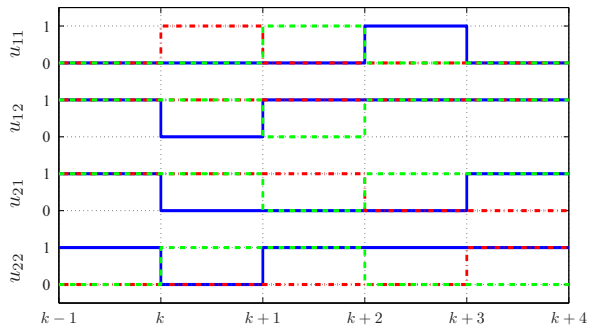

(b) Predicted switching sequences

Fig. 3: Three candidate switching sequences for a four step prediction horizon, i.e. $N = 4$.

Based on (10), (11), and (12) the objective function is chosen as

$$J(k) = \sum_{\ell=k}^{k+N-1} \Big(||i_{s,err}(\ell+1|k)||_1 + ||v_{o,err}(\ell+1|k)||_1 + q||\Delta u(\ell|k)||_1 \Big) , \quad (13)$$

which penalizes the evolution of the variables of concern over the finite prediction horizon N using the 1-norm (sum of absolute values). The weighting factor $q \in \mathbb{R}^+$ sets the trade-off between the current and the output voltage errors and the switching frequency. Some guidelines for tuning the weighting factor q are presented in [23].

The control input at time-instant kT_s is obtained by minimizing the objective function (13) over the optimization variable, which is the sequence of switching states over the horizon $U(k) = [u(k)\ u(k+1) \dots u(k+N-1)]^T$. Thus the following constrained optimization problem is formulated:

$$\begin{aligned} \underset{U}{\text{minimize}} \quad & J(k) \\ \text{subject to} \quad & \text{eq. (1)} . \end{aligned} \quad (14)$$

The underlying optimization problem is a mixed-integer non-linear optimization problem [24]. For solving such type of problems enumeration is a straightforward option. By taking into account all possible combinations of the switching states ($u_{ip} = 0$ or $u_{ip} = 1$) the switching sequences to be examined are created. The evolution of the state is calculated for each of the 2^{2nN} sequences and the objective function is evaluated. The sequence U^* with the smallest associated cost is considered as the optimal solution, given by

$$U^*(k) = \arg\min J(k) . \quad (15)$$

Out of this sequence, the first element $u^*(k)$ is applied to the converter; the procedure is repeated at $k+1$, based on new measurements acquired at the following sampling instance. An illustrative example of the predicted state – here the inductor current – and the sequence of the control actions, i.e. the switching state, is depicted in Fig. 3. Three candidate switching sequences are shown for the prediction horizon $N = 4$, and for a CHB rectifier consisting of two cells. In Fig. 3(a) the current of step k is the measured one, while from $k+1$ to $k+N$ the current evolution is depicted according to the switching sequences shown in Fig. 3(b).

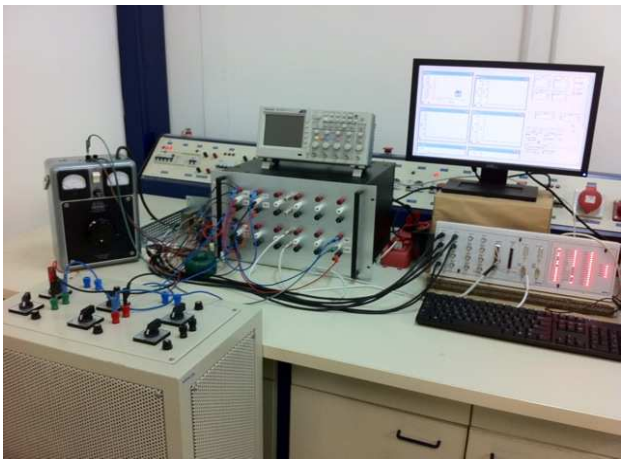

Fig. 4: Experimental setup that includes a prototype CHB rectifier (left – below the oscilloscope) and the dSpace real-time system used for control (right – below the monitor).

C. Outer Loop

The outer loop is used for the voltage regulation. A proportional-integral (PI) controller is employed – one for each cell – to regulate the respective output voltage to its reference value. The reference current $\hat{i}_{s,ref}$ derived, shown in Fig. 2, is further synchronized with the supply voltage by a phase lock loop (PLL), resulting in a sinusoidal reference current $i_{s,ref}$.

IV. Performance Evaluation

In this section experimental results of the proposed control algorithm are presented. As a case study a CHB single-phase rectifier consisting of two H-bridge cells is considered, i.e. as the one shown is Fig. 1 with $n = 2$, rated at 1 kW. The input voltage is $v_s = 110$ V, the nominal frequency $f = 50$ Hz, and the output voltage references are set equal for each cell $v_{o,ref_i} = 100$ V. The boost inductance is $L = 8$ mH, with internal resistance $R_L = 0.7\,\Omega$, and the filter capacitance is $C_{o_i} = 2.2$ mF.

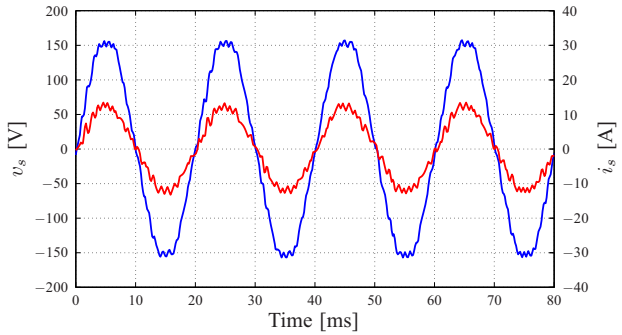

(a) Input voltage (blue line) and current (red line).

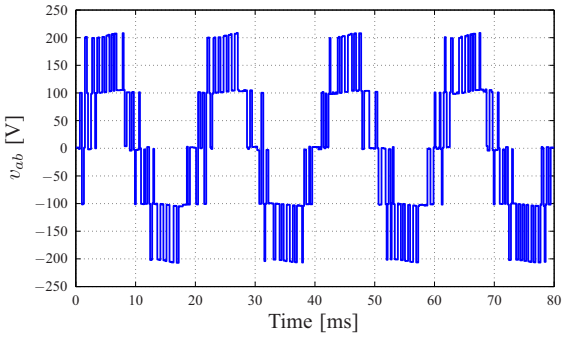

(b) AC side voltage.

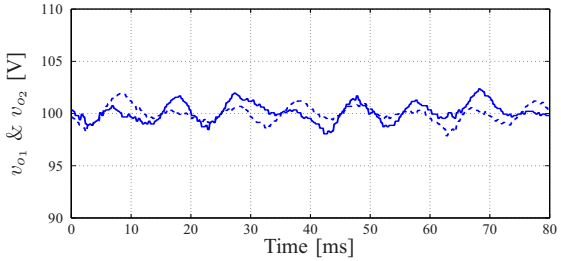

(c) Output voltage of first (solid line) and second cell (dashed line).

Fig. 5: Experimental results from a CHB single-phase rectifier consisting of two H-bridge cells operating in steady-state under nominal conditions.

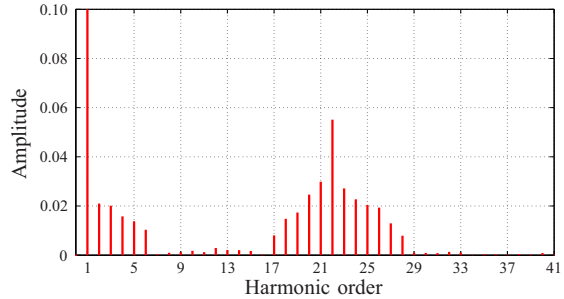

Fig. 6: Input current spectrum. The THD of the input current i_s is 3.27%. The current is given in p.u..

Regarding the controller parameters, the weight in the objective function (13) is heuristically chosen as $q = 0.2$, the prediction horizon is $N = 2$ and the sampling time is $T_s = 100\,\mu$s. The control algorithm was implemented on a dSpace 1104 system with I/O card for real-time control. The experimental setup is shown in Fig. 4.

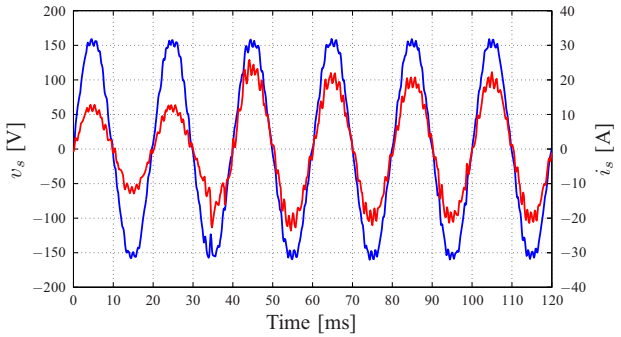

(a) Input voltage (blue line) and current (red line).

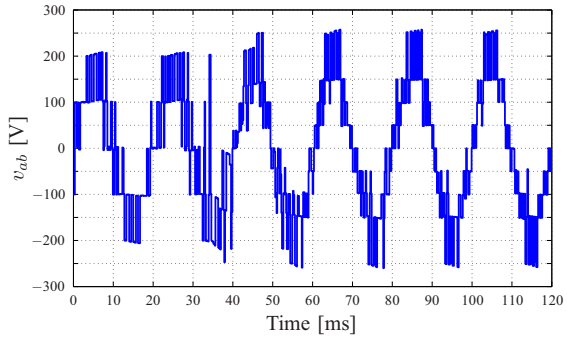

(b) AC side voltage.

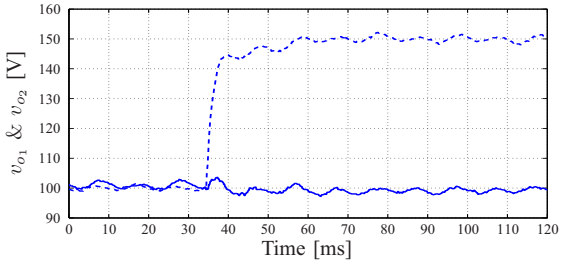

(c) Output voltage of first (solid line) and second cell (dashed line).

Fig. 7: Experimental results for a step-up change in the output voltage reference of the second cell.

A. Steady-State Operating Conditions

Initially the converter operates under nominal conditions with a switching frequency of about $f_{sw} = 1.1\,$kHz. The steady-state performance is examined and the results are presented in Fig. 5. As can been seen in Fig. 5(a) the input current i_s is a sinusoidal waveform and in phase with the supply voltage v_s. The harmonic content of the input current is low, resulting in a THD of 3.27%, according to Fig. 6 where the current spectrum up to the 41^{st} harmonic is depicted. It can be observed that the current spectrum is distributed around the 22^{nd} harmonic, i.e. the most significant harmonics are located in high frequencies corresponding to the switching frequency and the frequencies around it. In Fig. 5(b) the 5-Level reflected voltage to the AC side is illustrated, resulting from the fact that the two-cell converter is operating under balanced output cell voltages, i.e. the output voltage reference for both cells is

set equal to $v_{o,ref_1} = v_{o,ref_2} = 100\,\mathrm{V}$ (Fig. 5(c)).

B. Step Change in the Output Reference Voltage

Next, a step change in the reference of the output voltage of the second cell takes place (Fig. 7). At time $t \approx 35\,\mathrm{ms}$ the reference is stepped up from $v_{o,ref_2} = 100\,\mathrm{V}$ to $v_{o,ref_2} = 150\,\mathrm{V}$. The output voltage of the second cell reaches its new reference value in about $t \approx 25\,\mathrm{ms}$ without any overshoot or undershoot, while the output voltage of the first cell remains practically unaffected by this change (Fig. 7(c)). The input current response to the aforementioned change is depicted in Fig. 7(a); the amplitude instantaneously increases, while the unity power factor is maintained. Finally the AC side reflected multilevel voltage (Fig. 7(b)) is composed of nine distinctive levels due to the unbalanced output cell voltages, as it is expected.

V. Conclusions

In this work a model predictive control (MPC) approach for the cascaded H-bridge (CHB) multilevel rectifier based on enumeration is introduced. By directly manipulating the switches of the converter the regulation of the input current to its reference is achieved; the voltage term added in the objective function maintains the effectiveness of the strategy introduced when operating under unbalanced output cell voltages. The controller is able to stabilize the system for the entire operating regime due to the exhaustive search of all possible switching combinations. Furthermore, the proposed algorithm exhibits favorable performance during transients. In addition, the nature of the controller implies that it is directly extendable to other topologies such as the three-phase rectifier. These benefits overshadow the drawbacks of the proposed technique such as the increased computational complexity and the variable switching frequency resulting from the absence of a modulator. Finally, the performance of the presented control algorithm is verified by experimental results from a two-cell CHB single-phase multilevel rectifier.

References

[1] S. Vazquez, J. I. Leon, J. M. Carrasco, L. G. Franquelo, E. Galvan, M. Reyes, J. A. Sanchez, and E. Dominguez, "Analysis of the power balance in the cells of a multilevel cascaded H-bridge converter," *IEEE Trans. Ind. Electron.*, vol. 57, no. 7, pp. 2287–2296, Jul. 2010.

[2] D. G. Holmes and T. A. Lipo, *Pulse Width Modulation for Power Converters: Principles and Practice*. Piscataway, NJ, USA: IEEE Press, 2003.

[3] G. S. Konstantinou and V. G. Agelidis, "Performance evaluation of half-bridge cascaded multilevel converters operated with multicarrier sinusoidal PWM techniques," in *Proc. IEEE Conf. Ind. Electron. Appl.*, Xi'an, China, May 2009, pp. 3399–3404.

[4] J. I. Leon, S. Vazquez, A. J. Watson, L. G. Franquelo, P. W. Wheeler, and J. M. Carrasco, "Feed-forward space vector modulation for single-phase multilevel cascaded converters with any dc voltage ratio," *IEEE Trans. Ind. Electron.*, vol. 56, no. 2, pp. 315–325, Feb. 2009.

[5] S. Kouro, P. Lezana, M. Angulo, and J. Rodríguez, "Multicarrier PWM with dc-link ripple feedforward compensation for multilevel inverters," *IEEE Trans. Power Electron.*, vol. 23, no. 1, pp. 52–59, Jan. 2008.

[6] J. I. Leon, S. Vazquez, S. Kouro, L. G. Franquelo, J. M. Carrasco, and J. Rodríguez, "Unidimensional modulation technique for cascaded multilevel converters," *IEEE Trans. Ind. Electron.*, vol. 56, no. 8, pp. 2981–2986, Aug. 2009.

[7] J. I. Leon, S. Kouro, S. Vazquez, R. Portillo, L. G. Franquelo, J. M. Carrasco, and J. Rodríguez, "Multidimensional modulation technique for cascaded multilevel converters," *IEEE Trans. Ind. Electron.*, vol. 58, no. 2, pp. 412–420, Feb. 2011.

[8] A. X. Kaletsanos, I. S. Manolas, K. G. Pavlou, and S. N. Manias, "Sliding mode control for cascaded H-bridge boost rectifiers," in *Proc. IEEE Int. Symp. Ind. Electron.*, Bari, Italy, Jul. 2010, pp. 1070–1075.

[9] B.-R. Lin, H.-H. Lu, and S.-C. Tsay, "Control technique for high power factor multilevel rectifier," *IEEE Trans. Aerosp. and Electron. Sys.*, vol. 37, no. 1, pp. 226–241, Jan. 2001.

[10] H. Iman-Eini, J.-L. Schanen, S. Farhangi, and J. Roudet, "A modular strategy for control and voltage balancing of cascaded H-bridge rectifiers," *IEEE Trans. Power Electron.*, vol. 23, no. 5, pp. 2428–2442, Sep. 2008.

[11] C. Cecati, A. Dell'Aquila, M. Liserre, and V. G. Monopoli, "A passivity-based multilevel active rectifier with adaptive compensation for traction applications," *IEEE Trans. Ind. Appl.*, vol. 39, no. 5, pp. 1404–1413, Sep./Oct. 2003.

[12] A. J. Watson, P. W. Wheeler, and J. C. Clare, "A complete harmonic elimination approach to dc link voltage balancing for a cascaded multilevel rectifier," *IEEE Trans. Ind. Electron.*, vol. 54, no. 6, pp. 2946–2953, Dec. 2007.

[13] J. M. Maciejowski, *Predictive Control with Constraints*. Prentice-Hall, 2002.

[14] J. B. Rawlings and D. Q. Mayne, *Model Predictive Control: Theory and Design*. Madison, WI, USA: Nob Hill Publ., 2009.

[15] Y. A.-R. I. Mohamed and E. F. El-Saadany, "Robust high bandwidth discrete-time predictive current control with predictive internal model—A unified approach for voltage-source PWM converters," *IEEE Trans. Power Electron.*, vol. 23, no. 1, pp. 126–136, Jan. 2008.

[16] P. Cortés, J. Rodríguez, P. Antoniewicz, and M. Kazmierkowski, "Direct power control of an AFE using predictive control," *IEEE Trans. Power Electron.*, vol. 23, no. 5, pp. 2516–2523, Sep. 2008.

[17] J. Rodríguez, J. Pontt, C. A. Silva, P. Correa, P. Lezana, P. Cortés, and U. Ammann, "Predictive current control of a voltage source inverter," *IEEE Trans. Ind. Electron.*, vol. 54, no. 1, pp. 495–503, Feb. 2007.

[18] J. D. Barros and J. F. Silva, "Optimal predictive control of three-phase NPC multilevel converter for power quality applications," *IEEE Trans. Ind. Electron.*, vol. 55, no. 10, pp. 3670–3681, Oct. 2008.

[19] T. Geyer, G. Papafotiou, R. Frasca, and M. Morari, "Constrained optimal control of the step-down dc-dc converter," *IEEE Trans. Power Electron.*, vol. 23, no. 5, pp. 2454–2464, Sep. 2008.

[20] P. Cortés, A. Wilson, S. Kouro, J. Rodríguez, and H. Abu-Rub, "Model predictive control of cascaded H-bridge multilevel inverters," *IEEE Trans. Ind. Electron.*, vol. 57, no. 8, pp. 2691–2699, Aug. 2010.

[21] C. Townsend, T. J. Summers, and R. E. Betz, "Model predictive control of a cascaded H-bridge multi-level StatCom," in *Proc. IEEE Energy Convers. Congr. Expo.*, Atlanta, GA, USA, Sep. 2010, pp. 2133–2140.

[22] M. Vasiladiotis, K. Pavlou, S. Manias, and A. Rufer, "Model predictive-based control method for cascaded H-bridge multilevel active rectifiers," in *Proc. IEEE Energy Convers. Congr. Expo.*, Phoenix, AZ, USA, Sep. 2011, pp. 3200–3207.

[23] P. Cortés, S. Kouro, B. La Rocca, R. Vargas, J. Rodríguez, J. I. León, S. Vazquez, and L. G. Franquelo, "Guidelines for weighting factors design in model predictive control of power converters and drives," in *Proc. IEEE Int. Conf. Ind. Technol.*, Gippsland, Australia, Feb. 2009, pp. 1–7.

[24] A. Bemporad and M. Morari, "Control of systems integrating logic, dynamics and constraints," *Automatica*, vol. 35, no. 3, pp. 407–427, Mar. 1999.